Efficient Three-dimensional Imaging From a Small Cylindrical Aperture

Mark A. Haun[†]*, Douglas L. Jones, and William D. O'Brien, Jr.*

Department of Electrical and Computer Engineering
University of Illinois at Urbana-Champaign, Urbana, IL 61801

Abstract — Small-diameter cylindrical imaging platforms, like those being considered in the development of *in vivo* ultrasonic microprobes, pose unique image formation challenges. Their shape is incompatible with many of the commonly used frequency-domain synthetic aperture imaging algorithms, and their small diameter places limits on the available aperture and the angular resolution that may be achieved. A three-dimensional, frequency-domain imaging algorithm is obtained for this geometry by making suitable approximations to the point spread function in cylindrical coordinates and obtaining its Fourier transform by analogy with the equivalent problem in Cartesian coordinates. For the most effective use of aperture, we propose using a focused transducer to place a virtual source a short distance from the probe. The focus is treated as a real unfocused source by the imaging algorithm, which then forms images on deeper cylindrical shells. This approach retains the simplicity and potential angular resolution of a single element, yet permits full use of the available probe aperture and a higher energy output. Computer simulations and experimental results using wire targets show that this imaging technique attains the resolution limit dictated by the operating wavelength and the transducer characteristics.

I. INTRODUCTION

An ongoing research project at the University of Illinois is developing very small ultrasound transducers that can be fabricated on the side of a needle and operated *in vivo* at high frequencies. One long-term goal of this research is to supplement or even replace biopsy with a safer tool for tumor diagnosis. Crucial to the success of this effort are imaging algorithms adapted to the unique requirements of these ultrasonic microprobes.

This image formation problem is challenging due to the microprobes' shape. With one probe, only two transducer motions are possible: inward and outward travel, and rotation about the needle axis. Thus, besides the cylindrical geometry, there is the problem of limited aperture. Because the microprobe transducer will be immersed in a scattering volume, good resolution in three dimensions is desirable so that quality 2-D image slices may be obtained with synthetic aperture techniques. As this requires a significant 2-D aperture, it is imperative that the available probe diameter be used efficiently.

Many of these constraints also apply to other imaging systems. Some intra-vascular ultrasound (IVUS) systems, for example, use a circular array of transducers on a catheter to image the interior of blood vessels. As new ultrasound imaging modalities are developed, it is anticipated that cylindrical apertures will become more common and will benefit from ongoing work in this area.

Supported by NIH Grant CA79179

II. SYNTHETIC APERTURE IMAGING IN A CYLINDRICAL GEOMETRY

Circular apertures have previously been used for intravascular ultrasound (IVUS) imaging systems, where synthetic aperture or array focusing has usually been carried out in the time domain [1, 2]. Frequency-domain algorithms, however, have a large speed advantage over traditional beamforming methods due to the computational efficiency of the Fast Fourier Transform.

A frequency-domain imaging method was recently proposed for use with IVUS systems. The authors start with a geometrically derived, two-dimensional point spread function (PSF) and obtain the Fourier transform of the imaging kernel for monostatic and bistatic cases using the method of stationary phase [3, 4].

In the following derivation, the PSF for three-dimensional, monostatic imaging from a cylindrical aperture is obtained using the Rayleigh-Sommerfeld formulation of scalar diffraction theory. This PSF is then compared with the PSF for wave propagation in Cartesian coordinates, which has a well-known Fourier transform. This approach makes clear the approximations necessary to put the PSF for cylindrical coordinates into the same form and obtain its Fourier transform.

We start with the Rayleigh-Sommerfeld formula [5],

$$U(P_0) = \int\int_{\Sigma} \frac{1}{j\lambda} U(P_1) \frac{e^{jkr_{01}}}{r_{01}} \cos(\vec{n}, \vec{r}_{01}) ds \qquad (1)$$

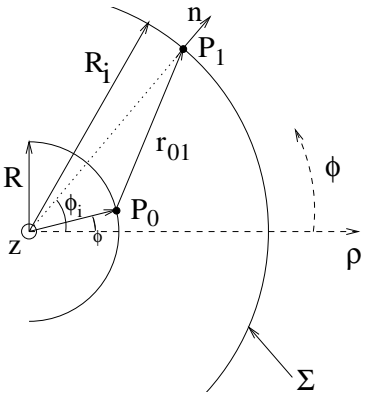

Figure 1: Cylindrical geometry for derivation of the point-spread function (PSF).

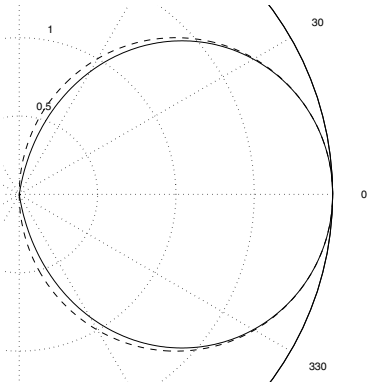

Figure 2: Circles of constant travel time for exact (dashed line) and approximate (solid line) forms of the distance function.

which expresses the signal at P_0, located on the imaging aperture, in terms of a source distribution on the surface Σ shown in Figure 1. No generality is lost by assuming that the scatterers on Σ are themselves the source of ultrasonic waves traveling at speed $c/2$. This is the "exploding reflectors" model common in seismic exploration. In cylindrical coordinates we have

$$U(R,\phi,z) = \int_{-\infty}^{\infty}\int_{-\pi}^{\pi} \frac{1}{j\lambda} U(R_i,\phi_i,z_i) \cdot \frac{\exp(jk\sqrt{R^2+R_i^2-2RR_i\cos(\phi-\phi_i)+(z-z_i)^2})}{R^2+R_i^2-2RR_i\cos(\phi-\phi_i)+(z-z_i)^2} \cdot (R_i - R\cos(\phi-\phi_i))R_i d\phi_i dz_i \quad (2)$$

This is a convolution integral; the point spread function is

$$h(\phi,z) = \frac{1}{j\lambda}(R_i - R\cos\phi)R_i \cdot \frac{\exp(jk\sqrt{R^2+R_i^2-2RR_i\cos\phi+z^2})}{R^2+R_i^2-2RR_i\cos\phi+z^2} \quad (3)$$

If the transducer beamwidth is not too wide, the cosine terms in the exponential and the denominator may be approximated to second order $(1-\phi^2/2)$. If the other cosine term in the numerator is approximated to first order, we have

$$h(\phi,z) \approx \frac{1}{j\lambda}(R_i - R)R_i \cdot \frac{\exp(jk\sqrt{(R-R_i)^2+RR_i\phi^2+z^2})}{(R-R_i)^2+RR_i\phi^2+z^2} \quad (4)$$

The square-root quantity in (2) that is being approximated is the distance from the transducer to a reflector in the scattering volume, expressed in cylindrical coordinates. Figure 2 shows (in a 2-D projection) sample loci of constant travel time for both the approximate and exact distance formulas for a transducer at $R=1$, $\phi=0$. This illustrates the limits of the small beamwidth assumption.

Now compare the approximated $h(\phi,z)$ with the PSF obtained for a rectangular aperture in Cartesian coordinates:

$$h(x,y) = \frac{1}{j\lambda}\cdot\frac{d\exp(jk\sqrt{d^2+x^2+y^2})}{d^2+x^2+y^2} \quad (5)$$

Clearly they have the same form, except that the angular variable is scaled by the geometric mean of the transducer and reflector radii. The Fourier transform of $h(x,y)$ is well known, and the transform of $h(\phi,z)$ follows easily using the scaling property:

$$H(f_\phi,f_z) \approx \sqrt{\frac{R_i}{R}}\, e^{j2\pi(R_i-R)\sqrt{\frac{1}{\lambda^2}-\frac{f_\phi^2}{RR_i}-f_z^2}} \quad (6)$$

where the fact that ϕ is an angular variable (and $h(\phi,z)$ is thus periodic in ϕ) has been ignored, and $\lambda = c/2f$ in accordance with the exploding reflectors model.

In the spatial-frequency (f_ϕ, f_z) domain, multiplication by H is equivalent to "propagating" the wave field from one concentric cylindrical surface to another. This is the principle behind what are known as migration algorithms in the seismic exploration community and wavenumber or $\omega-k$ algorithms in the radar community [6]. A simple way to obtain a two-dimensional image is as follows [7]:

1. Take 3-D FFT of the raw data: $(\phi,z,t) \rightarrow (f_\phi,f_z,f)$
2. Multiply the (f_ϕ,f_z) spatial frequency planes at each f by $H(f_\phi,f_z)$ for the target reconstruction depth
3. Average over temporal frequency f
4. Take the inverse 2-D FFT, yielding the focused image

Computer simulations were performed to verify the performance of this image formation algorithm. Five point-reflectors in an "X" pattern at radius R_i = 15 mm were imaged using an infinitesimally small, unfocused transducer

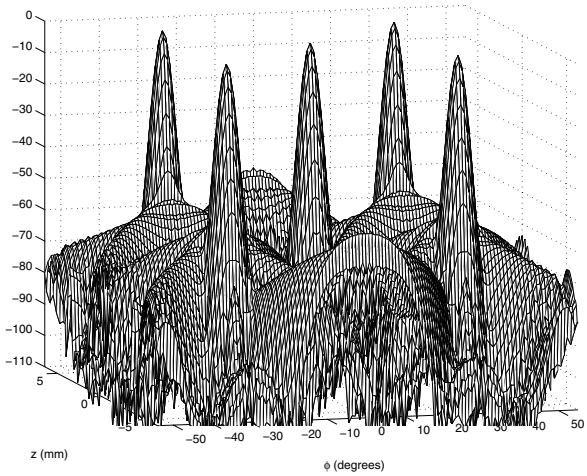

Figure 3: Reconstructed, log-scaled image for simulation with five point-reflectors.

at radius R = 8 mm and having a Gaussian beam shape with a -3 dB beamwidth of 20°. A Gaussian-weighted sinusoid with center frequency 5 MHz and bandwidth roughly 3 MHz was used as the pulse shape. Simulated echoes were collected on a 128x128 grid with ϕ ranging from -55° to $+55^\circ$ and z ranging from -6.4 to $+6.4$ mm. This data was processed with the algorithm described above; Figure 3 shows the results. The highest side lobes are about 50 dB down, and the synthesized half-power beamwidth at the reflectors is less than λ.

III. OPTIONS FOR EFFECTIVE USE OF THE AVAILABLE APERTURE

It is well known that the best lateral (azimuth or along-track) resolution available with synthetic aperture processing is approximately $D/2$, where D is the effective aperture of the antenna or transducer, which is assumed larger than a wavelength (see for example [8]). For high-frequency ultrasound applications, this would seem to suggest using a transducer that is extremely small, on the order of one wavelength! This may be possible in practice, but the small transducer size places a severe limit on the available pulse energy in an application where the low signal-to-noise ratio is already a major concern.

One possible solution is to use the full probe diameter for a focused transducer and treat the focus as a virtual source. The virtual source then traces out a surface larger than the probe, as shown in Figure 4. The imaging algorithm proceeds as if there were an unfocused transducer located at the focus and forms images at depths beyond that point. A recent study exploring this technique found that

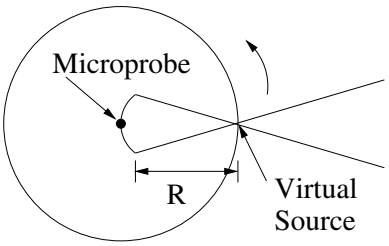

Figure 4: Using a focused transducer to create a virtual source element.

the resolution achievable past the focus is comparable to the resolution at the focus [9].

Using a focused transducer to create a virtual source has the advantage that more transducer area, and hence more energy, is available for transmitting. It is important to realize, however, that there is no "free lunch" here: the usable aperture is still the same, even though the virtual source may be traveling on a much larger surface. Assuming a constant transducer diameter, as the focal length is increased, the width of the focal region increases and the beamwidth past the focus decreases. These factors conspire to keep the best attainable resolution about the same for either approach.

IV. EXPERIMENTAL RESULTS

To test the validity of the proposed frequency-domain imaging algorithm in conjunction with the virtual source technique, experiments were performed in a water tank with a precision positioning and data acquisition system. A 15-MHz transducer having a 12.7-mm diameter, 19.1-mm focal length, and theoretical resolution at focus of $\lambda D/F = 150$ μm was mounted to a vertical support arm. The target was a piece of aluminum wire mesh held at constant radius from the support arm and about 5 mm beyond the focus of the transducer (see Figure 5). The transducer was scanned up and down and rotated about the axis of the support arm, covering an area of 6.4 mm by 8.32° in 128 by 128 steps.

Figure 6 shows two log-scaled images of the wire mesh, at distances of 5.17 mm and 5.30 mm beyond the focus of the transducer. The mesh consists of vertical wires which are nearly straight, parallel, and normal to the view direction, and horizontal wires which weave through them. The upper image shows some of the vertical wires and also the over-crossings of the horizontal wires. In the lower image, the deeper focus reveals other vertical wires, indicating that the wire mesh was not held precisely at a constant radius. Most of the wire over-crossings are still visible, but the rest of the horizontal wires remain invisible due to their angles with respect to the view direction (note that the wire diameter, at 280 μm, is larger than the acoustic wavelength).

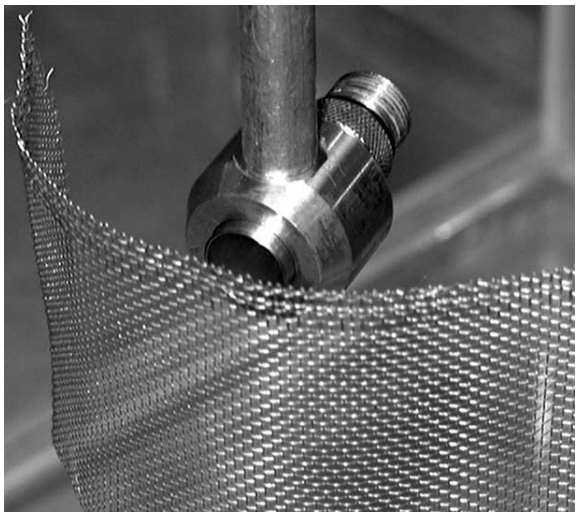

Figure 5: Experimental set-up showing transducer and wire mesh phantom.

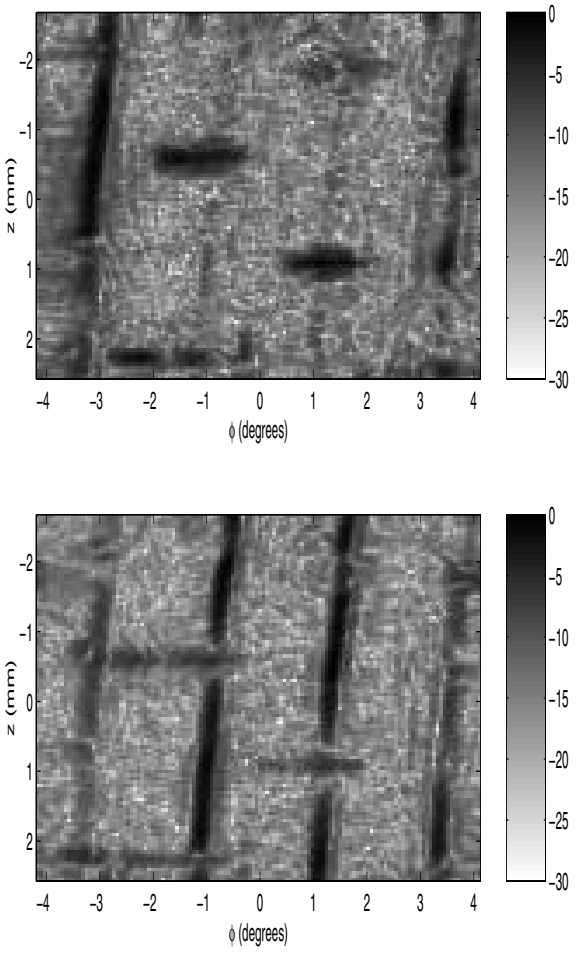

Figure 6: Reconstructed images of wire mesh at 5.17 mm (top) and 5.30 mm (bottom) beyond the transducer's focus.

V. CONCLUSIONS

An efficient and accurate three-dimensional image formation algorithm has been obtained directly through simple approximations to the point spread function for 3-D wave propagation in cylindrical coordinates. Computer simulations and experimental results verify its good performance. When combined with the virtual source technique, this algorithm should allow high quality, near-diffraction-limited imaging from small cylindrical platforms, whether they be needles, catheters, or others yet to be developed.

VI. REFERENCES

[1] M. O'Donnell, "Efficient synthetic aperture imaging from a circular aperture with possible application to catheter-based imaging," *IEEE Trans. UFFC*, vol. 39, no. 3, pp. 366–380, May 1992.

[2] M. O'Donnell, "Synthetic phased arrays for intraluminal imaging of coronary arteries," *IEEE Trans. UFFC*, vol. 44, no. 3, pp. 714–721, May 1997.

[3] T. Rastello, C. Haas, D. Vray, M. Krueger, K. Schroeder, E. Brusseau, G. Gimenez, and H. Ermert, "A new Fourier-based multistatic synthetic aperture focusing technique for intravascular ultrasound imaging," in *Proc. IEEE Ultrason. Symp.*, Toronto, Canada, October 1998, pp. 1725–1728.

[4] C. Haas, M. Krueger, H. Ermert, D. Vray, G. Gimenez, W. Bojara, and J. Barmeyer, "Beam compression of multistatic intravascular ultrasound data by an adaptive kernel function," in *Proc. IEEE Ultrason. Symp.*, Lake Tahoe, Nevada, October 1999, pp. 1283–1286.

[5] J.W. Goodman, *Introduction to Fourier Optics*, McGraw-Hill, New York, second ed., 1996.

[6] C. Cafforio, C. Prati, and E. Rocca, "SAR data focusing using seismic migration techniques," *IEEE Trans. on Aero. and Elec. Sys.*, vol. 27, no. 2, pp. 194–206, March 1991.

[7] L.J. Busse, "Three-dimensional imaging using a frequency-domain synthetic aperture focusing technique," *IEEE Trans. UFFC*, vol. 39, no. 2, pp. 174–179, March 1992.

[8] D.C. Munson, Jr. and R.L. Visentin, "A signal processing view of strip-mapping synthetic aperture radar," *IEEE Trans. Acoustics, Speech, and Sig. Proc.*, vol. 37, no. 12, pp. 2131–2147, December 1989.

[9] C.H. Frazier and W.D. O'Brien, Jr., "Synthetic aperture techniques with a virtual source element," *IEEE Trans. UFFC*, vol. 45, no. 1, pp. 196–207, January 1998.

† Email correspondence to markhaun@uiuc.edu